Near surface westerly wind jet in the Atlantic ITCZ

Semyon A. Grodsky, James A. Carton, and Sumant Nigam
Department of Meteorology University of Maryland College Park, Maryland, USA

Received 30 May 2003; revised 1 July 2003; accepted 23 July 2003; published 3 October 2003.

[1] A suite of satellite data are used to study the near surface westerly winds developing during peak months (July–September) of the West African monsoon in the Atlantic Intertropical Convergence Zone. These new data show that the westerlies appear in the form of a westerly jet. During peak years the daily near-surface westerly wind speed may exceed 10 ms^{-1}. The amplitude of the jet displays substantial decadal and interannual variability that corresponds to rainfall in the West African Sahel and the frequency of African Easterly Waves. Observations and ocean model simulations show that the jet acts to cool SST through entrainment and latent heat loss and to intensify the North Equatorial Countercurrent by increasing the southward oceanic pressure gradient. *INDEX TERMS:* 3374 Meteorology and Atmospheric Dynamics: Tropical meteorology; 4231 Oceanography: General: Equatorial oceanography; 4275 Oceanography: General: Remote sensing and electromagnetic processes (0689); 4279 Oceanography: General: Upwelling and convergences; 4504 Oceanography: Physical: Air/sea interactions (0312). **Citation:** Grodsky, S. A., J. A. Carton, and S. Nigam, Near surface westerly wind jet in the Atlantic ITCZ, *Geophys. Res. Lett.*, *30*(19), 2009, doi:10.1029/2003GL017867, 2003.

1. Introduction

[2] Atmospheric circulation over West Africa during the boreal summer is strongly affected by the development of a pressure trough in the lower atmosphere over the Sahara. This Sahara pressure trough contrasts with the relatively higher pressure over the Gulf of Guinea and Sahel. The resulting mostly meridional pressure gradient drives shallow westerly monsoon flow in northern summer [*Carlson*, 1969]. Field studies during the Global Atmospheric Research Program Atlantic Tropical Experiment showed these shallow westerly winds are contained inside the frictional boundary layer (depth of ~2km) and within the latitude band between 0° to 20°N. They attain maximum speeds of 5 ms^{-1} at ~8°N [*Reed et al.*, 1977].

[3] In this study we exploit the improved spatial and temporal resolution of satellite data to provide further details on the shallow westerly winds over the ocean in the latitude band of the Intertropical Convergence Zone (ITCZ). We then examine the impact of these westerlies on the surrounding ocean using observations and numerical simulations.

2. Data

[4] This study is based on joint examination of satellite winds, rainfall, sea surface temperature (SST), sea surface height, surface drifter currents, and reanalysis winds and pressure. Winds have been measured by the SeaWinds scatterometer aboard the QuikSCAT satellite [*Graf et al.*, 1998]. Rainfall is based on a combination of the TRMM Microwave Imager, and the Precipitation Radar aboard the US/Japanese Tropical Rainfall Measuring Mission (TRMM) satellite [see *Kummerow et al.*, 2000 and citations there]. SST has been obtained from the *Reynolds and Smith* [1994] blended satellite–in situ analysis. Sea surface height has been obtained from the TOPEX/POSEIDON altimetry Pathfinder archive (*Koblinsky*, personal communication, 1997). Winds at fixed pressure levels and sea level pressure are provided by the National Centers for Environmental Prediction/National Center for Atmospheric Research (NCEP/NCAR) reanalysis of *Kalnay et al.* [1996]. Ocean near surface drifter currents are provided by the GOOS Center at the Atlantic Oceanographic and Meteorological Laboratory/NOAA.

3. Results

[5] During boreal summer intense surface heating over the Sahara is associated with a decrease in atmospheric pressure. The resulting meridional gradient in surface pressure turns both northern and southern trade winds towards the continent, resulting in the West African monsoon. Westerly winds appear most strongly where the two trade wind systems converge. A daily snapshot in Figure 1a shows a westerly wind jet exceeding 15 ms^{-1} at some locations and extending across the whole basin. Westerly winds appear beginning in May and persist through September (see Figure 1b) with their latitudinal position following the meridional migration of the ITCZ. They are also subject to substantial quasi-biweekly oscillations previously noted by *Janicot and Sultan* [2001] and *Grodsky and Carton* [2001].

[6] In addition to strong seasonal and intraseasonal variability, the westerlies are subject to significant year-to-year changes as well with stronger westerlies in the summer of 1999 than 2000 (Figure 2). The change in winds between these two summers is reflected in the westward extension of the Sahara pressure trough over the ocean. We find that a simple linear three-term momentum balance relating pressure gradients, Rayleigh friction, and the Coriolis term [*Deser*, 1993; *Chung et al.*, 2002] provides a reasonable description of zonal winds associated with the westerly jet (using zonal/meridional Rayleigh friction coefficients 10^{-5} $s^{-1}/2 \times 10^{-5}$ s^{-1} as suggested by *Chiang and Zebiak* [2000]) (Figure 1c) to within the uncertainties in the pressure and wind estimates.

[7] Next we consider the observed year-to-year variability through an Empirical Orthogonal Function analysis of the NCEP/NCAR reanalysis late-boreal-summer zonal

0094-8276/03/2003GL017867$05.00

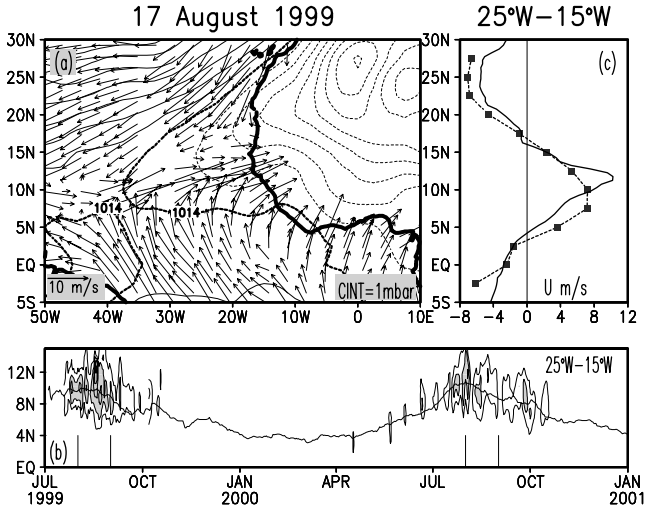

Figure 1. (a) QuikSCAT winds on 17 August 1999 and the NCEP/NCAR mean sea level pressure. (c) Observed (solid) and calculated (symbols, see paragraph [6]) zonal wind averaged 25°W–15°W. (b) Latitude-time diagram of the QuikSCAT zonal winds averaged 25°W–15°W. The latitude of the strongest wind convergence is shown as a proxy for the ITCZ position. Only the eastward zonal wind isolines are drawn at [2.5, 5, 7.5, 10, 12.5] ms^{-1}. Wind exceeding 5 ms^{-1} is shaded. Vertical lines show the beginning and end of each August.

winds over the central tropical Atlantic (Figure 3a). This analysis shows that the westerly wind jet is the near surface expression of westerly winds that reach their maximum at ~700 mb [see also *Reed et al.*, 1977]. During years with stronger near-surface westerly winds stronger zonal wind shear develops in the lower troposphere that horizontal favors the development of African Easterly Waves. This relationship is demonstrated in Figure 3b by comparing zonal winds with the African Easterly Wave index of *Thorncroft and Hodges* [2001]. Since the African Easterly Waves are occasionally predecessors of tropical storms and hurricanes of the western Atlantic [*Carlson*, 1969], the decadal variation of the westerly wind amplitude (shown in Figure 3b) corresponds to the decadal variation of Atlantic hurricane activity including the decrease between 1950s through 1980s and the increase during the 1990s.

[8] The monsoon winds bring humid maritime air and thus rainfall to the Sahel. This relationship was demonstrated by *Grist and Nicholson* [2001] who have found stronger low-level westerly winds during the "wet" years in the Western Sahel (and vice-versa). Similarly, *Jury et al.* [2002] have found a relationship between zonal winds in the central Atlantic (10°S–5°N, 40°W–0°E) and African rainfall. Our data in Figure 3b also suggest a substantial relationship between the amplitude of the westerly wind jet and the Western Sahel Rainfall Index of *Lamb* [1983; and personal communication, 2002]. The relationship improves after the 1960s, possibly because of improvements in the observing system.

[9] Next we consider how the ocean responds to the westerly wind jet. The near surface westerly wind jet causes enhanced positive wind curl to the north and negative curl to the south leading to corresponding anomalies of Ekman pumping. To evaluate the importance of this effect, we examine the difference in Ekman pumping (computed from scatterometer winds), sea surface height, SST, and surface currents (Figure 4) between August 1999 and August 2000 (years of strong and weak westerly winds, respectively). Upward Ekman pumping velocity, w_e, along 10°N (Figure 4a) was stronger during 1999 by at least 0.25 m day^{-1}. This strengthening results in thermocline shallowing and causes a corresponding drop in sea surface height of at least −3 cm (Figure 4b). The change in the meridional difference in sea surface height across the latitude of the ITCZ is at least $\delta\eta$ = 6 cm. This change also intensifies the North Equatorial Countercurrent that flows eastward following isolines of sea surface height. If we assume a mixed layer depth of h ~70 m at 5°N [following *White*, 1995], then a sea surface height anomaly of 6 cm distributed between the equator and 10°N increases the eastward geostrophic transport by $gf^{-1}\delta\eta h = 3.2 \times 10^6$ m^3s^{-1} or ~15% of the total North Equatorial Countercurrent transport [*Katz*, 1993]. Surface drifter currents in Figure 4d are also consistent with a strengthened North Equatorial Countercurrent in August 1999 relative to August 2000.

[10] Monthly mean wind velocity in August 1999 relative to August 2000 displays significant eastward difference of

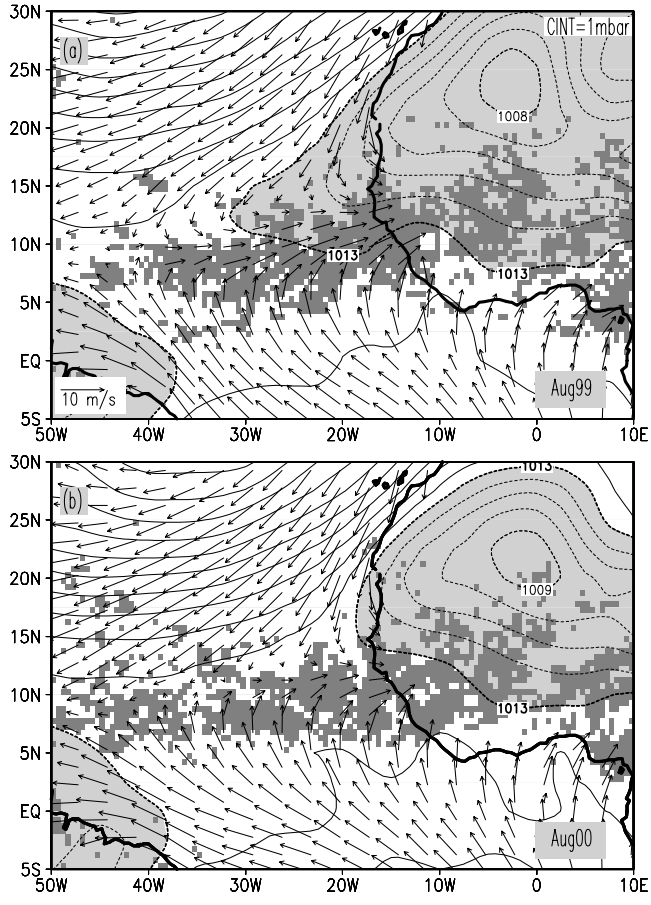

Figure 2. August mean QuikSCAT winds, NCEP/NCAR reanalysis mean sea level pressure, and TRMM rainfall in (a) 1999 and (b) 2000. The 1013 mb and minimum pressure contours over Sahara are labeled. Pressure lower than 1013 mb is shaded. Rainfall exceeding 0.25 mm hr^{-1} is shown in dark gray.

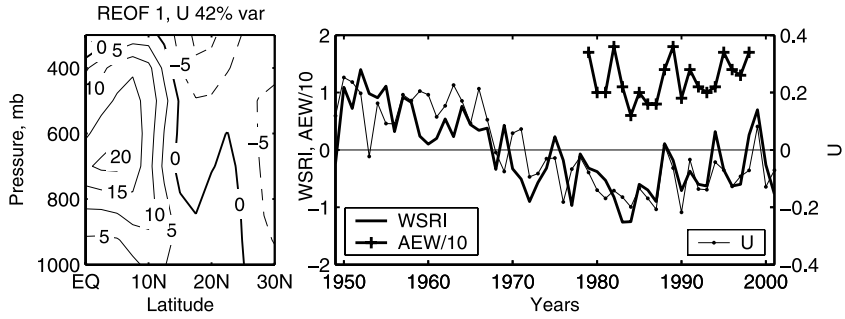

Figure 3. (a) First rotated Empirical Orthogonal Function of the August zonal winds averaged 30°W to 10°W. (b) Time series of first EOF amplitude (U), number of African Easterly Waves (AEW) of *Thorncroft and Hodges* [2001], and the Western Sahel Rainfall Index ($WSRI$) of *Lamb* [1983]. Temporal correlation $\langle U, WSRI \rangle = 0.78$.

$\sim$5 ms^{-1} in magnitude (Figure 4e) due to the intense westerly wind jet in 1999. Because of the change in direction the difference in speed is $\sim$2 ms^{-1}. If we assume that the mixed layer temperature anomaly is due to entrainment and latent cooling only, the anomaly ocean mixed layer temperature budget simplifies to

$$h\frac{d\delta \mathrm{SST}}{dt} = w_e \Delta T - \frac{a\delta W}{C_p \rho} \qquad (1)$$

where $h \sim 40$ m at this latitude (10°N), the temperature discontinuity at the base of the mixed layer $\Delta T \sim 0.75$°C [following *Swenson and Hansen*, 1999], and the linearized latent heat flux resulting from a wind speed change (δW) is $a = 6.5$ Jm^{-3} (assuming SST = 28°C and relative humidity $q = 90\%$). Integrating (1) over a month (the characteristic timescale of these anomalies) for $w_e \sim 0.3$ m day^{-1} gives the entrainment contribution to SST cooling of -0.15°C and the latent heat flux contribution -0.2°C for $\delta W = 2$ ms^{-1}. The total SST cooling due to both mechanisms of ~ -0.3°C is consistent with observed cooling of SST (Figure 4c).

[11] To further explore the ocean's response to anomalous winds we turn to a general circulation model configured for the tropical Atlantic. The model is based on the Geophysical Fluid Dynamics Laboratory/NOAA Modular Ocean Model (version 2) physics (see *Carton et al.*, 1996 for model details and simulations of interannual SST variabilty), and is forced by QuikSCAT winds and a surface temperature boundary condition relaxing toward the year 2000 observed SST (with a 50-day relaxation time-scale). The control simulation consists of forcing the model with year 2000 winds (weak westerly) repeatedly for five years beginning from climatological temperature and salinity conditions. The experiment consists of modifying the winds during July–September of the sixth year by adding the 1999 minus 2000 wind differences (strong westerly) in the ITCZ belt bounded by a Gaussian filter centered at 30°W, 9°N with 30° longitude and 3° latitude spatial scales (see Figure 5a).

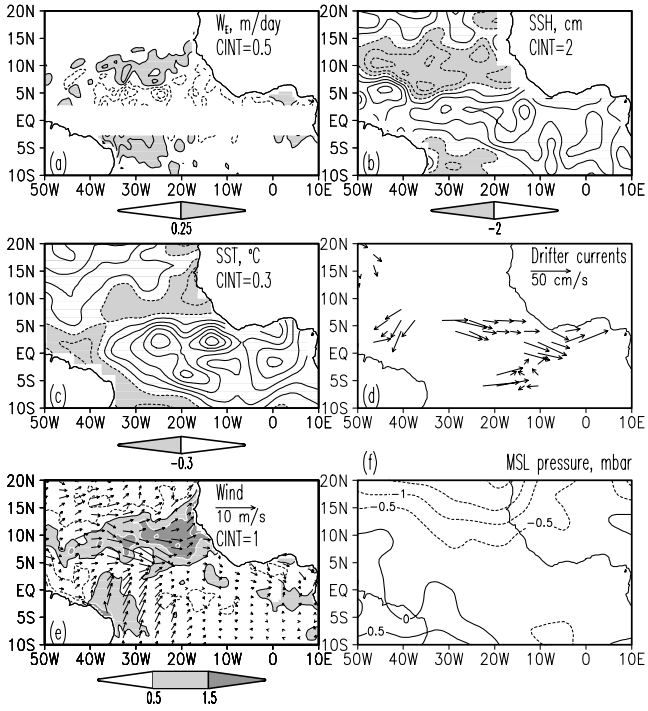

Figure 4. 1999 minus 2000 observed differences during August. (a) Ekman pumping velocity (positive - upward). (b) Sea surface height. (c) Sea surface temperature. (d) Drifter surface currents. (e) Wind velocity (arrows) and wind speed (contours). Contours are drawn at [−1.5, −0.5, 0.5, 1.5, 2.5] ms^{-1}. Wind speed increase exceeding 0.5 ms^{-1} is shaded. (f) Mean sea level pressure.

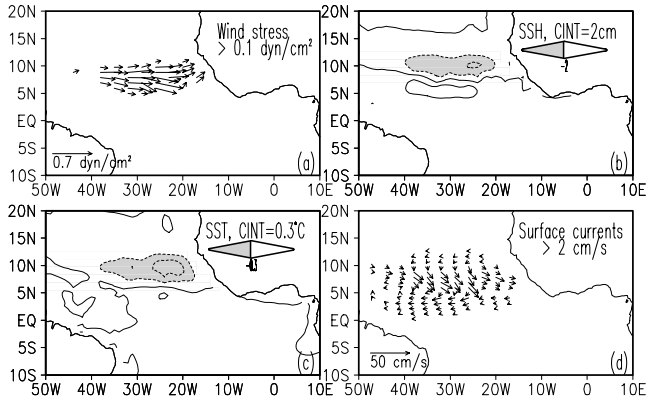

Figure 5. 1999 minus 2000 simulated differences during August. (a) Wind stress (only values exceeding 0.1 dyn cm^{-2} in magnitude are shown). (b) Sea surface height. (c) Sea surface temperature. (d) Surface currents (only values exceeding 2 cm s^{-1} in magnitude are shown).

The spatial and temporal bounding of the wind difference eliminates the Atlantic Niño warming (see *Carton et al.*, 1996 for further details) and concentrates on the dynamical effect of the westerly wind jet upon the ocean. The experiment is compared with the fifth year of the control simulation.

[12] In general agreement with observations, the experiment shows stronger upward pumping to the north and stronger downward pumping to the south of the westerly wind jet that results in an increase in the meridional gradient of sea surface height (Figure 5b) and a strengthening of the North Equatorial Countercurrent. There are several areas of disagreement between the observations and experiment as well. The simulated increase of the zonal current ($\sim$10 cm s^{-1}, Figure 5d) is roughly half that observed by the drifters ($\sim$20 cm s^{-1}, Figure 4d). The simulated current has a southward component that is not observed. The simulated SST decrease ~ -0.6°C (Figure 5c) is stronger than the $\sim$0.3°C observed (Figure 4c) because of the increase in southward current.

4. Discussion and Conclusion

[13] QuikSCAT scatterometer winds indicate that a strong near surface westerly wind jet develops in the Atlantic ITCZ. The monthly mean wind speed in this jet during late boreal summer could exceed 7 ms^{-1}. During this time it extends well into the central basin between 40°W and the African coast. The jet also shows strong intraseasonal variability. During peak years the daily near surface westerly wind speed may exceed 10 ms^{-1}.

[14] The westerly wind jet strengthens the meridional gradient of Ekman pumping. This causes cooling of the mixed layer and shallowing of the thermocline to the north and warming and deepening to the south. The associated changes in the meridional gradient of sea surface height could intensify the eastward North Equatorial Counter Current transport by around 15%. Intensification of the winds also causes an increase in latent heat loss. We compare the Ekman pumping and latent heat loss effects during 2000 relative to 1999 and find they have similar impact on reducing SST.

[15] The westerly jet is in near-geostrophic balance with the meridonal atmospheric pressure gradient set up by the Sahara trough extension. This relationship leaves us with the question of what mechanisms regulate the southward extension of the Sahara trough over the ocean and its year-to-year variation. *Tomas and Webster* [1997] have argued that the near surface westerly jet could result from the clockwise turning of the southern trades after their entry into the northern latitudes if a southward cross-equatorial pressure gradient exists. By considering the nonlinear vorticity balance, they have found that the low-level westerlies should increase north of the zero absolute vorticity line. But this mechanism doesn't explain what causes the extension in the Sahara trough and the southward pressure gradient. A more complete examination of this question will likely require a fully coupled model.

[16] **Acknowledgments.** This work was supported by NOAA's Offices of Oceanic and Atmospheric Research and Global Programs and by the National Science Foundation. We appreciate comments from Peter Lamb who also has provided an update of the West Sahel Rainfall Index. We are grateful to Xianhe Cao for assistance in running the ocean model. Drifter data has been obtained from the Drifter DAC of the GOOS Center at NOAA/AOML. QuikSCAT wind has been obtained from the NASA/NOAA sponsored system Seaflux at JPL through the courtesy of W. Timothy Liu and Wenqing Tang. Suggestions of anonymous reviewers were useful and stimulating.

References

Carlson, T. N., Synoptic histories of three African disturbances that developed into Atlantic hurricanes, *Mon. Wea. Rev.*, *97*, 256–276, 1969.

Carton, J. A., X. H. Cao, B. S. Giese, and A. M. daSilva, Decadal and interannual SST variability in the tropical Atlantic Ocean, *J. Phys. Oceanogr.*, *26*(7), 1165–1175, 1996.

Chiang, J. C. H., and S. E. Zebiak, Surface wind over tropical oceans: Diagnosis of the momentum balance, and modeling the linear friction coefficient, *J. Clim.*, *13*, 1733–1747, 2000.

Chung, C., S. Nigam, and J. A. Carton, SST-forced surface wind variability in the tropical Atlantic: An empirical model, *J. Geophys. Res.*, *107*(D15), doi:10.129/2001JD000324, 2002.

Deser, C., Diagnosis of the surface momentum balance over the tropical Pacific ocean, *J. Clim.*, *6*, 64–74, 1993.

Graf, J., C. Sasaki, C. Winn, W. T. Liu, W. Tsai, M. Freilich, and D. Long, NASA Scatteromometer Experiment, *Acta Astronautica*, *43*, 397–407, 1998.

Grist, J. P., and S. E. Nicholson, A study of the dynamics factors influencing the rainfall variability in the West African Sahel, *J. Clim.*, *14*, 1337–1359, 2001.

Grodsky, S. A., and J. A. Carton, Coupled land/atmosphere interactions in the West African Monsoon, *Geophys. Res. Lett.*, *28*, 1503–1506, 2001.

Janicot, S., and B. Sultan, Intra-seasonal modulation of convection in the West African monsoon, *Geophys. Res. Lett.*, *28*, 523–526, 2001.

Jury, M. R., D. B. Enfield, and J.-L. Melice, Tropical monsoon around Africa: Stability of ENSO associations and links with continental climate, *J. Geophys. Res.*, *107*(C10), 3151, doi:10.129/2000JC000507, 2002.

Kalnay, E., Coauthors, The NCEP/NCAR 40-year reanalysis project, *Bull. Amer. Meteorol. Soc.*, *77*, 437–471, 1996.

Katz, E. J., An interannual study of the Atlantic North Equatorial Countercurrent, *J. Phys. Oceanogr.*, *23*, 116–123, 1993.

Kummerow, C., Coauthors, The Status of the Tropical Rainfall Measuring Mission (TRMM) after Two Years in Orbit, *J. Applied Meteor.*, *39*, 1965–1982, 2000.

Lamb, P., Sub-Saharan rainfall update for 1982: Continued drought, *J. Climatol.*, *3*, 419–422, 1983.

Reed, R. J., D. C. Norquist, and E. E. Recker, The structure and properties of African disturbances as observed during phase III of GATE, *Mon. Wea. Rev.*, *105*, 317–333, 1977.

Reynolds, R. W., and T. M. Smith, Improved global sea surface temperature analyses using optimum interpolation, *J. Clim.*, *7*, 929–948, 1994.

Swenson, M. S., and D. V. Hansen, Tropical Pacific ocean mixed layer heat budget: The Pacific Cold Tongue, *J. Phys. Oceanogr.*, *29*, 69–81, 1999.

Thorncroft, C., and K. Hodges, African easterly wave variability and its relationship to Atlantic tropical cyclone activity, *J. Clim.*, *14*, 1166–1179, 2001.

Tomas, R. A., and P. J. Webster, The role of internal variability in determining the location and strength of near-equatorial convection, *Quart. J. Roy. Meteor. Soc.*, *123*, 1445–1482, 1997.

White, W. B., Design of a global observing system for gyre-scale upper ocean temperature variability, *Progress in Oceanogr.*, *36*, 169–217, 1995.

S. A. Grodsky, J. A. Carton, and S. Nigam, Department of Meteorology University of Maryland College Park, MD 20742, USA. (senya@atmos.umd.edu; carton@atmos.umd.edu; nigam@atmos.umd.edu)